8 The intermetallic diffusion mechanism in composite Pd membranes

8.1 Introduction

Intermetallic diffusion is the migration of the elements in the porous metal support (mostly Fe, Cr and Ni) into the Pd layer, thereby affecting the H_2 permeance of the membrane. Intermetallic diffusion can be mitigated by forming or depositing an oxide or a high melting point metal layer on the porous metal support. Intermetallic diffusion barriers (also named thermal barrier coatings) can be formed by oxidation in air (Akis et al., 2003; Ma et al., 2004; Ma et al., 1998; Ma et al., 2000), deposition of nickel particles coated by a sol gel γ -Al_2O_3 layer (Nam and Lee, 2001), sandwiching of an Al_2O_3 foil (Edlund and McCarthy, 1995; Edlund and Pledger, 1993, 1994), deposition of tungsten or tantalum oxide (Gryaznov et al., 1993) and titanium nitride (Nam and Lee, 2005; Shu et al., 1996).

Metallic atoms start to acquire sufficient mobility at temperatures close to half of the material's melting point in Kelvin. 316L PSS supports melt at 1375-1400ºC, hence at 500-550ºC metallic atoms in the PSS support start to acquire enough mobility to diffuse into the Pd layer. Therefore, the H_2 permeance in composite Pd-PSS membranes should start to decrease at temperatures close to 500ºC. However, H_2 flux decline was observed in composite Pd-oxidized PSS membranes at temperatures as low as 275-350ºC

(Rothenberger et al., 2004). The diffusion of Fe, Cr and Ni into the Pd lattice, and vice versa, takes place at a very slow rate if not at all at 300ºC. Therefore, other processes such as: grain boundary diffusion of Fe, Cr or Ni in between the Pd grains, Pd clusters and grain growth, reduction of surface oxides with subsequent grain boundary diffusion of reduced elements into the Pd layer might lead to the decrease in H_2 permeance observed by many researchers at low temperatures (275-350º).

The activation energy for H_2 permeation through Pd-Fe or Pd-Cr alloys is higher than the activation energy for H_2 permeation through pure Pd (Flanagan et al., 1977; Swansiger et al., 1976). Therefore, intermetallic diffusion in composite Pd-PM support membranes should lead to an increase of the activation energy for H_2 permeation.

The main objective of this chapter was to understand the underlying mechanisms leading to the H_2 permeation loss in composite Pd-PM supports membranes at low and high temperatures. The capability of oxides formed on PM supports by air oxidation to mitigate or inhibit intermetallic diffusion in Pd-oxidized PM membranes was also investigated. Finally, a kinetic approach was undertaken to study the diffusion mechanism of the elements from the PM support into the Pd layer.

8.2 Experimental

Composite Pd membranes studied in this chapter are listed in Table 8-1. Membranes designated as C01-F0i were prepared according to the procedure described in Chapter 3 on oxidized PSS supports. Membranes designated as Ma-ii were prepared on "graded" PH supports. PH supports were graded with Pd seeds pre-activated Al_2O_3 powder following the experimental protocol described in Chapter 3 Section 3.1.2. The synthesis of C01-F06 was terminated since the deposition of as much as 19 μm of Pd only led to a very

small decrease of the original He permeance of the support, which was an indication of defects in the support. Therefore, the membrane was cut in several rings for the study of the oxide layer formed at 600ºC in air. Samples from C01-F06 were annealed in H_2 atmosphere at 300, 400, 500 and 600ºC for 48 hr.

Table 8-1 Characteristics of membranes studied in this chapter.

Membrane	Support Grade (μm)	O.D. (cm)	Length (cm)	Mem. Surf. [(a)] (cm^2)	Ox. Temp. (ºC)	Ox. Time (hr)	L (μm)
C01-F03	0.1 PSS	1.27	2.54	8.4	400	10	32
C01-F04	0.1 PSS	1.27	2.54	8.4	-	-	27
C01-F05	0.1 PSS	1.27	2.54	8.4	500	10	33
C01-F06[(b)]	0.1 PSS	1.27	6.35	23	600	10	19
C01-F07	0.1 PSS	1.27	6.35	23	500	10	23
Ma-32b	0.1 PH	2.54	15.24	120	700	12	10
Ma-34b	0.1 PH	2.54	15.24	120	700	12	8
Ma-42	0.1 PH	2.54	15.24	120	700	12	5.6

[(a)] The membrane surface area does not match the calculated surface using support OD and length due to the fact that the weld area for all membranes was taken as around $2cm^2$ of the porous area.
[(b)] C01-F06 was not a dense membrane. The synthesis was stopped due to large defects in the support. The membrane was cut in several pieces to study the structure of the oxide formed at 600ºC and its stability at different temperatures.

8.3 Results and discussion

8.3.1 The oxidation of porous metal supports

8.3.1.1 Oxide structure upon heating

After heating in air, the color of PSS supports changed from silver to gold when oxidized at 400ºC, to green when oxidized at 500ºC, to red-purple when oxidized 600ºC and to grey when oxidized at 800ºC. Each color responded to a different oxide structure. Oxidizing 316L PSS supports at 600ºC for 12 hr led to a thin, 0.8μm in thickness, oxide layer, which appeared as a dark layer in the SEM micrographs.

Figure 8-1(a) shows the cross-section of C01-F06 sample after heat-treatment at 300ºC under H_2 atmosphere for 48 hr. The elemental composition of the oxide layer was determined with EDX. Figure 8-1(b) shows four distinctive zones: (I) the stainless steel, (II) a chromium rich layer on the stainless steel, (III) an iron rich layer on top of the chromium oxide ("iron shoulder") and (IV) the Pd layer. The chromium and iron rich layers were obviously oxide layers since oxygen was also present. Oxidizing at 600ºC in stagnant air led to a thin (0.5-0.8μm) oxide layer, which consisted of a chromium oxide layer (0.1-0.2μm) and an iron oxide layer on top (0.4-0.6μm). The oxide layer was not uniform throughout the sample. The oxide structure found upon heating at 600ºC in air was in agreement with the oxide structure found by Ma et al. (2004).

The oxidation of 316L PSS at 400ºC and 500ºC led to oxide layers, which were too thin to be visible by SEM techniques and/or analyzed by EDX techniques. Therefore, the nature and the structure of oxides formed on PSS support upon heating at low temperatures could not be investigated. Yet, the green color of the 500ºC oxidized 316L PSS supports (for instance C01-F07's support after oxidation) suggested the presence of Cr_2O_3. Hence the structure of a composite Pd membrane prepared on a PSS support oxidized at temperatures higher than or equal to 600ºC was Pd-Fe_2O_3-Cr_2O_3-PSS. The structure of a composite Pd membrane prepared on a PSS support oxidized at temperatures lower than or equal to 500ºC was most probably Pd-Cr_2O_3-PSS. The Cr_2O_3 layer formed at low temperatures (<500ºC) was most probably thinner than 0.1-0.2 μm.

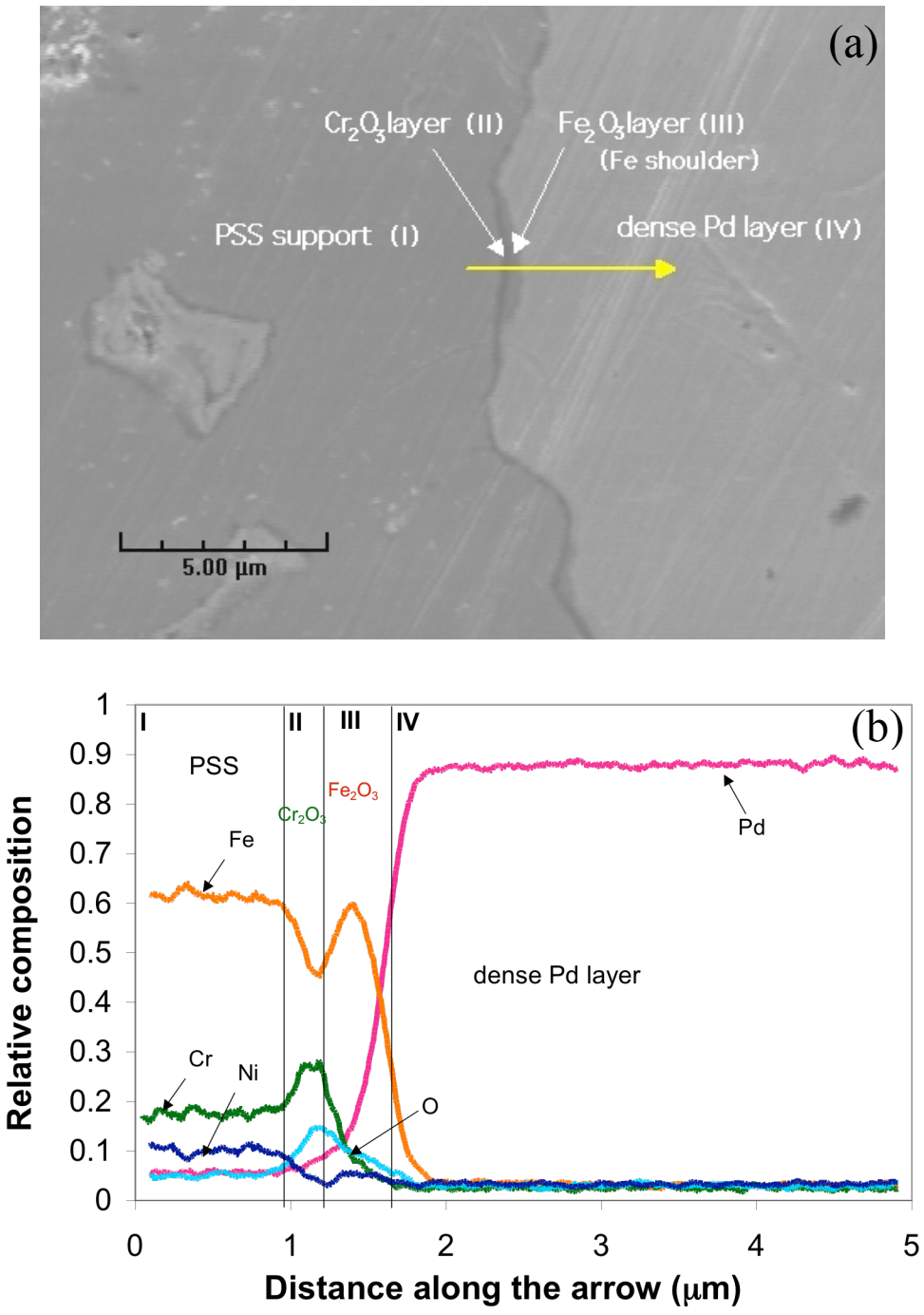

Figure 8-1 (a) SEM micrograph of the Pd-600ºC oxidized PSS interface. (b) Elemental composition across the Pd-oxidized PSS interface.

The oxidation of PH supports for membrane preparation was only conducted at 700ºC and led to a decrease in He permeance of 40-50 % of the initial He permeance. The oxidation at higher temperatures of PH supports for membrane application would have resulted in the complete clogging of the support's porosity. The oxide layer formed at 700ºC was thin and only Cr_2O_3 was detected with EDX. PH plates were oxidized at 900ºC for 12 hr to understand whether PH also has a tendency to form Fe_2O_3 on top of Cr_2O_3 as 316 L stainless steel does.

The crystallographic structure of Fe_2O_3, Cr_2O_3 and all Fe-Cr mixed oxides is very similar and their XRD patterns are therefore also very similar. The XRD pattern of Fe_2O_3 oxide has distinctive reflections ($I/I_0 > 30$) at $2\theta \approx 24.138$, 33.152, 35.611, 49.479, 54.089, 62.449 and 63.994º. The XRD pattern of Cr_2O_3 oxide has the same distinctive reflections with a slight shift to right: 24.496, 33.597, 36.196, 50.219, 54.853, 63.448 and 65.108º. The XRD reflections of all Fe-Cr mixed oxides lie between the XRD reflections of Fe_2O_3 and Cr_2O_3 with peak positions depending on the Fe/(Fe+Cr) ratio. Figure 8-2 shows the XRD pattern of the oxide layer formed after oxidation at 900ºC for 12 hr in stagnant air (316L PSS (blue peaks) and PH (green peaks)). Figure 8-2 (a), (b) and (c) show the XRD spectra in the low 2θ region, medium 2θ region and high 2θ region respectively. Figure 8-2 also shows the characteristic reflections of Fe_2O_3, Cr_2O_3 and $NiCrO_3$ references. The XRD pattern of the PSS support oxidized at 900ºC for 12 hr revealed the presence of Fe_2O_3 at the surface of the sample in agreement with the Fe_2O_3-Cr_2O_3-PSS structure found using EDX technique.

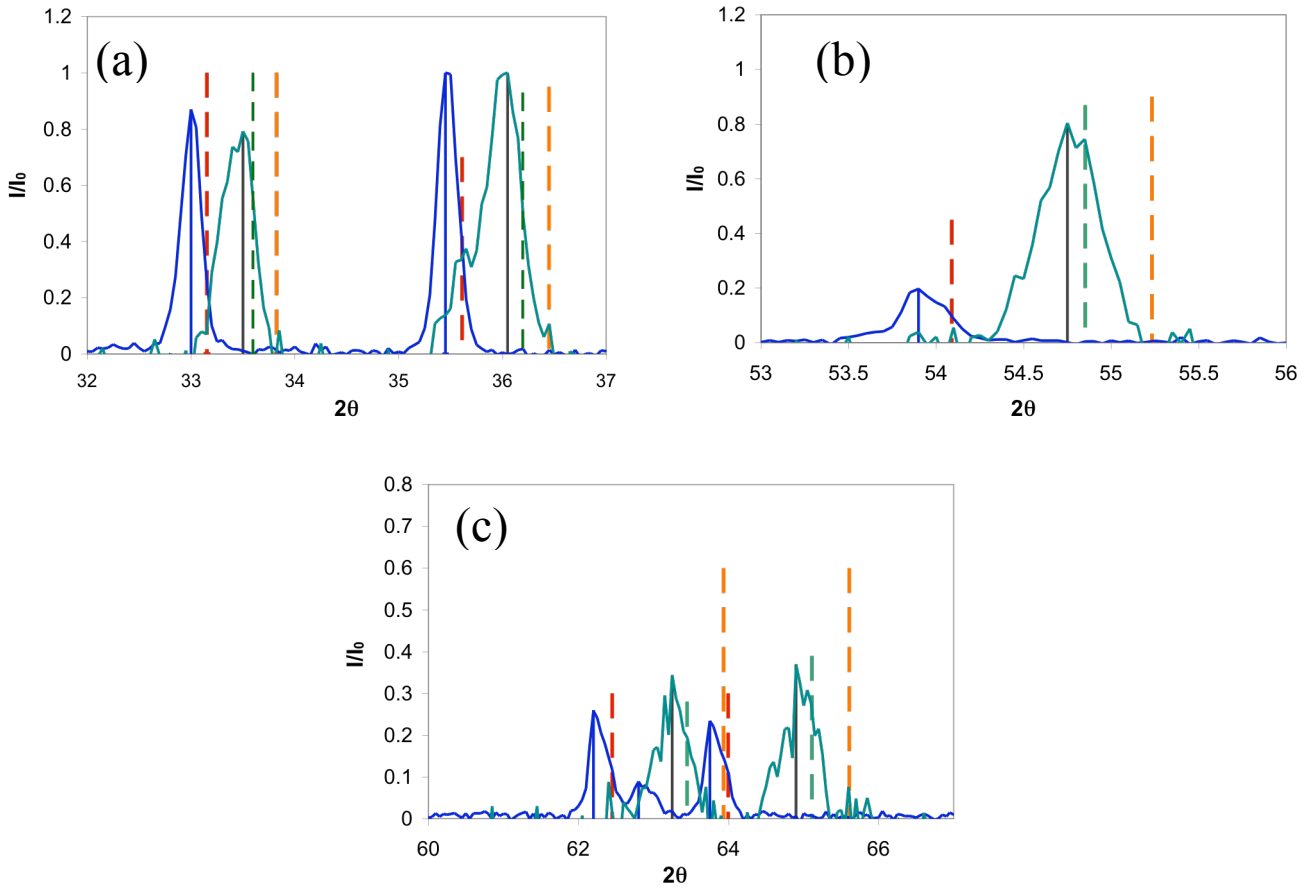

Figure 8-2 XRD spectra of PSS (blue) and PH (green) oxidized at 900ºC for 12 hr. (a) low 2θ range, (b) medium 2θ range and (c) high 2θ range. The reference XRD peaks of Fe_2O_3 (red dashed lines), Cr_2O_3 (green dashed lines) and $NiCrO_3$ (orange dashed lines) are also plotted for peak matching.

Moreover, the XRD peaks from the support were not detectable after oxidation indicating the formation of a very thick Fe_2O_3 layer (>5μm). The XRD pattern of the oxidized PH sample had the characteristic reflection of the support indicating that the oxide layer formed on PH samples upon oxidation at 900ºC for 12 hr was in the order of a micron (1-2μm). The XRD peaks of the oxide formed on PH were located to the right of the XRD peaks of the oxide formed on PSS at the same conditions. Therefore, oxides formed on PH were richer in Cr_2O_3. In fact, the XRD pattern of oxidized PH corresponded to the XRD pattern of the Cr_2O_3 reference.

The small shifts in both experimental Fe_2O_3 and Cr_2O_3 patterns were due to errors in sample height position. Since PH had up to 65wt% of Ni, Ni-rich oxide layers can be formed after oxidation. The presence of Ni-rich oxide layers was disregarded since the reference XRD peaks of $NiCrO_3$ laid far from the experimental oxide peaks.

PH has a tendency to develop thicker Cr_2O_3 oxide layers than 316L PSS. Moreover, no Fe_2O_3 layer was found on the outer surface of oxidized PH at high temperatures (900ºC) opposite to the oxidation of PSS samples.

8.3.1.2 Oxide stability in reducing atmosphere

The stability of the oxide layer formed on 316L PSS after heat-treatment at 600ºC was investigated by studying the cross-section of C01-F06 samples annealed at 400 and 500ºC in H_2 for 48 hr. The oxide layer formed at 600ºC was still visible after annealing at 400ºC in H_2 atmosphere as seen in Figure 8-3(a). Figure 8-3(b) shows the iron concentration profile of six different line-composition scans (lines 1 to 6) across the stainless steel-Pd interface of the 400ºC-annealed sample.

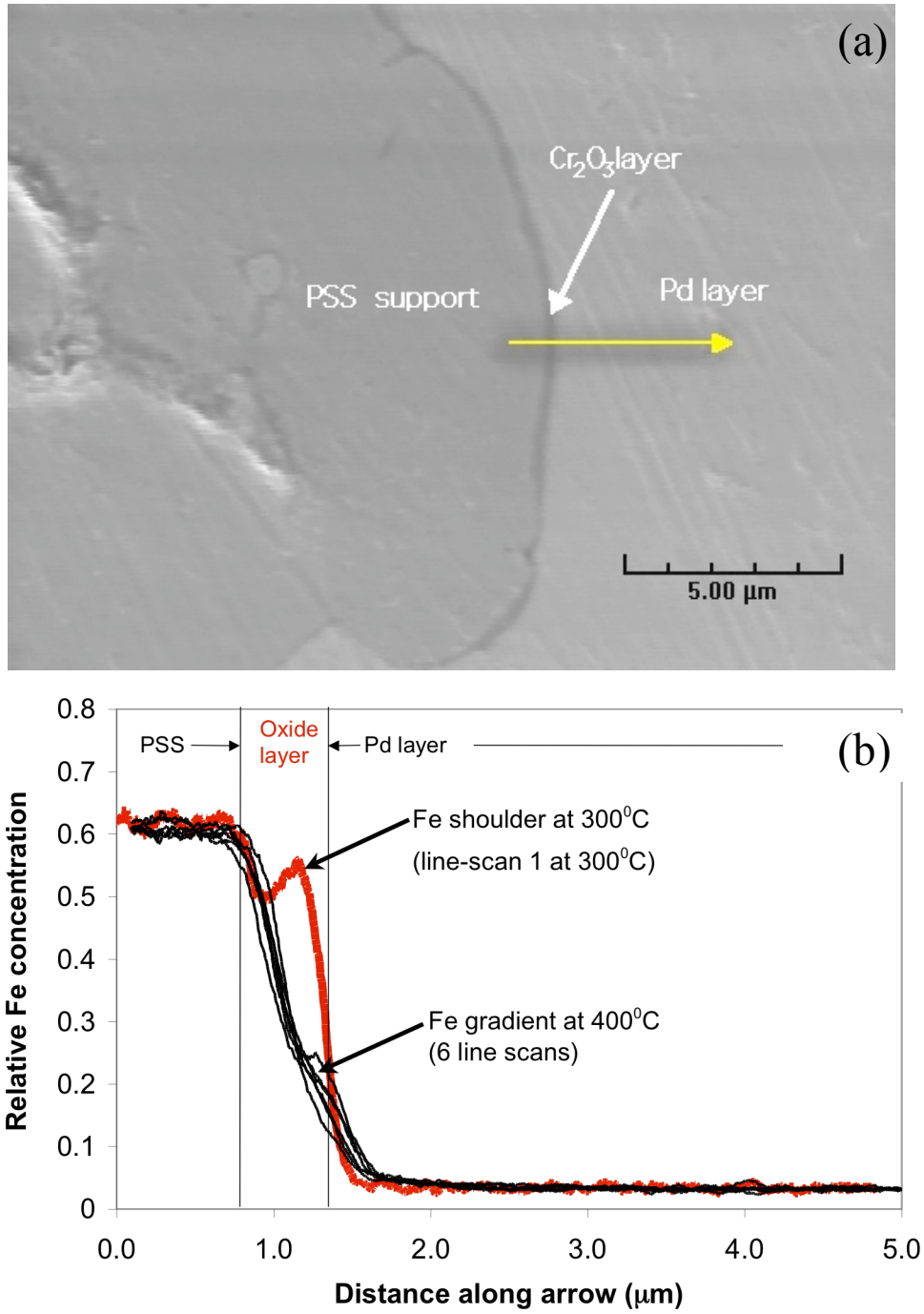

Figure 8-3 (a) SEM photograph of the Pd-oxidized PSS interface after heat-treatment at 400ºC in H_2 (b) Fe concentration across the steel-Pd interface for the sample annealed at 400ºC in H_2 for 48 hr at 6 different locations in the sample (line-scans 1-6). One of the scans (line-scan 1) of the sample at 300ºC was added for comparison.

The line-composition scan 1 from the 300ºC-annealed sample was superimposed for comparison purposes. In all scans performed on the 400ºC-annealed sample no iron oxide shoulders were detected but a gradient between the Fe content in the support (63wt%) and the Fe content of the Pd layer adjacent to the PSS support (0wt%). All scans, 1 through 6, can be considered as a single line scan as seen in Figure 8-3(b). It appeared that the reduction of the Fe_2O_3 layer took place at 400ºC when H_2 was dissolved in the Pd layer. The reduced Fe slightly diffused into the Pd layer leading to the Fe gradient seen in Figure 8-3(b).

Figure 8-4 (a) and (b) show a SEM micrograph of the oxide after heat-treatment at 500ºC in H_2 and the iron concentration profile across the interface respectively. At 500ºC, the thickness of the initial oxide layer dramatically decreased and a non-uniform gray layer was seen instead. The gray layer resulted from the inter-diffusion between the Pd layer and the support. No iron shoulders were detected but iron traces were measured up to 2μm in the Pd. Hence, at 500ºC the reduced iron readily diffused into the Pd layer.

A fourth sample of C01-F06 membrane was heat-treated at 600ºC for 48 hr in H_2. Figure 8-5(a) shows the SEM micrograph of the Pd-oxidized PSS interface after heat-treatment at 600ºC. Due to the intermetallic diffusion of Fe, the non-uniform grey layer visible at 500ºC grew thicker and corresponded to the diffusion of Pd into the stainless steel. Also, a thin oxide layer was still visible and appeared as a dark gray line in Figure 8-5(a). The Pd layer at the vicinity of the support was characterized by a darker color, due to the diffusion of Fe into the Pd layer. Figure 8-5(b) shows the Pd, Fe, Cr and Ni profile across the interface.

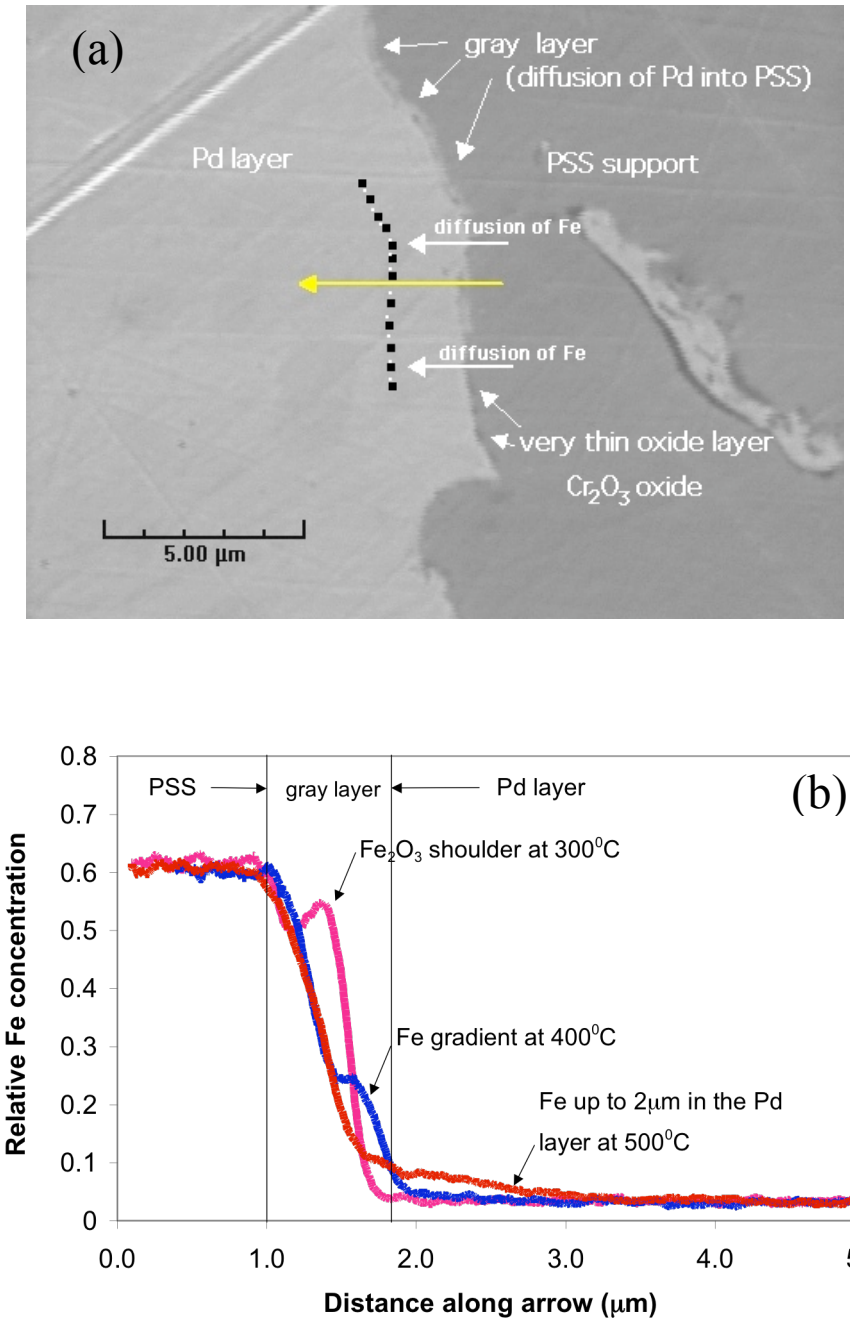

Figure 8-4 (a) SEM photograph of the Pd-oxidized PSS interface after heat-treatment at 500ºC in H_2 (b) Fe concentration profile of samples from C01-F06 annealed at 300ºC, 400ºC and 500ºC under H_2 atmosphere.

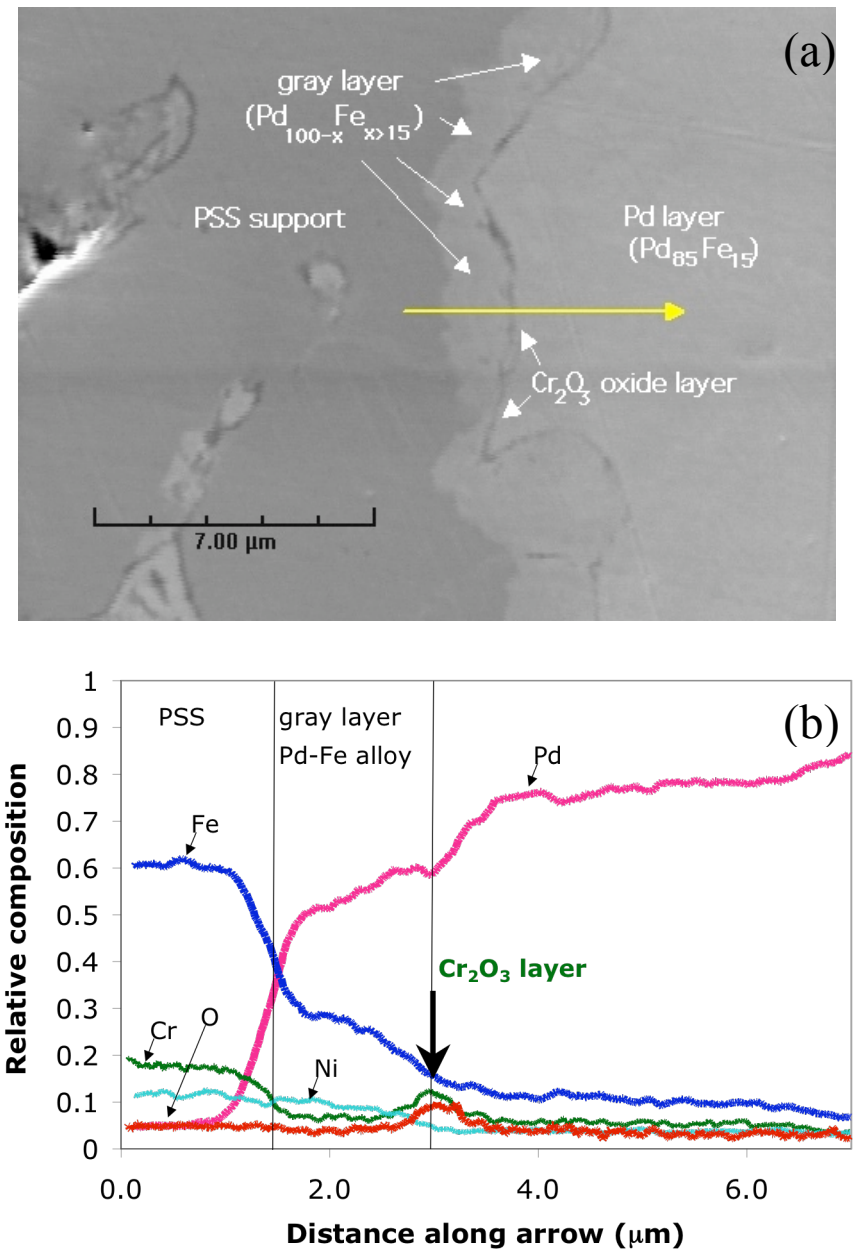

Figure 8-5 (a) SEM photograph of the Pd-oxidized PSS interface after heat-treatment at 600°C in H_2 (b) Fe, Pd, Cr and Ni concentration profile across the interface.

Large amounts of Pd diffused into the stainless steel and traces of Fe were detected up to 4 μm inside the Pd layer. Interestingly, the Cr concentration profile was characterized by a small peak, which corresponded to the thin dark grey layer still visible between the thick region where Pd diffused into the stainless steel and the Pd layer. Therefore, the thin 0.1-0.2 μm Cr_2O_3 layer resulting from the oxidation at 600ºC in air was not reduced when the composite Pd-oxidized PSS structure was in H_2 atmosphere at 600ºC. Figure 8-5(b) also shows that intermetallic diffusion was mostly the diffusion of Fe and some Cr into the Pd layer. Ni diffusion into the Pd layer was not observed.

The stability and ability of oxides formed on porous PH to suppress intermetallic diffusion was studied with a cross section sample of membrane Ma-34b. Figure 8-6 (a) shows the cross-section of Ma-34b after H_2 characterization at 600ºC. The distinctive gray layer of Cr_2O_3 was still present. Also, Pd diffused across the Cr_2O_3 porous layer into the PH forming a thin light grey region behind the Cr_2O_3 layer. The elemental composition across the Pd-oxidized PH interface is shown in Figure 8-6 (b). A Cr peak corresponding to the Cr_2O_3 layer was present at the Pd-PH interface. Pd diffused deep (up to 2μm) into the hastelloy grain, however, hardly any Ni or Cr was detected in the Pd layer. No large Fe concentrations were detected since PH had only 2-3wt% Fe.

The amount of intermetallic diffusion at 600ºC in H_2 atmosphere was significantly less in the Pd-PH system than in the Pd-PSS system. The reasons for such a strong ability of oxidized PH supports to prevent intermetallic diffusion was due to the fact that PH had a tendency to form a thicker Cr_2O_3 layer without any Fe_2O_3 formed on top the Cr_2O_3 layer.

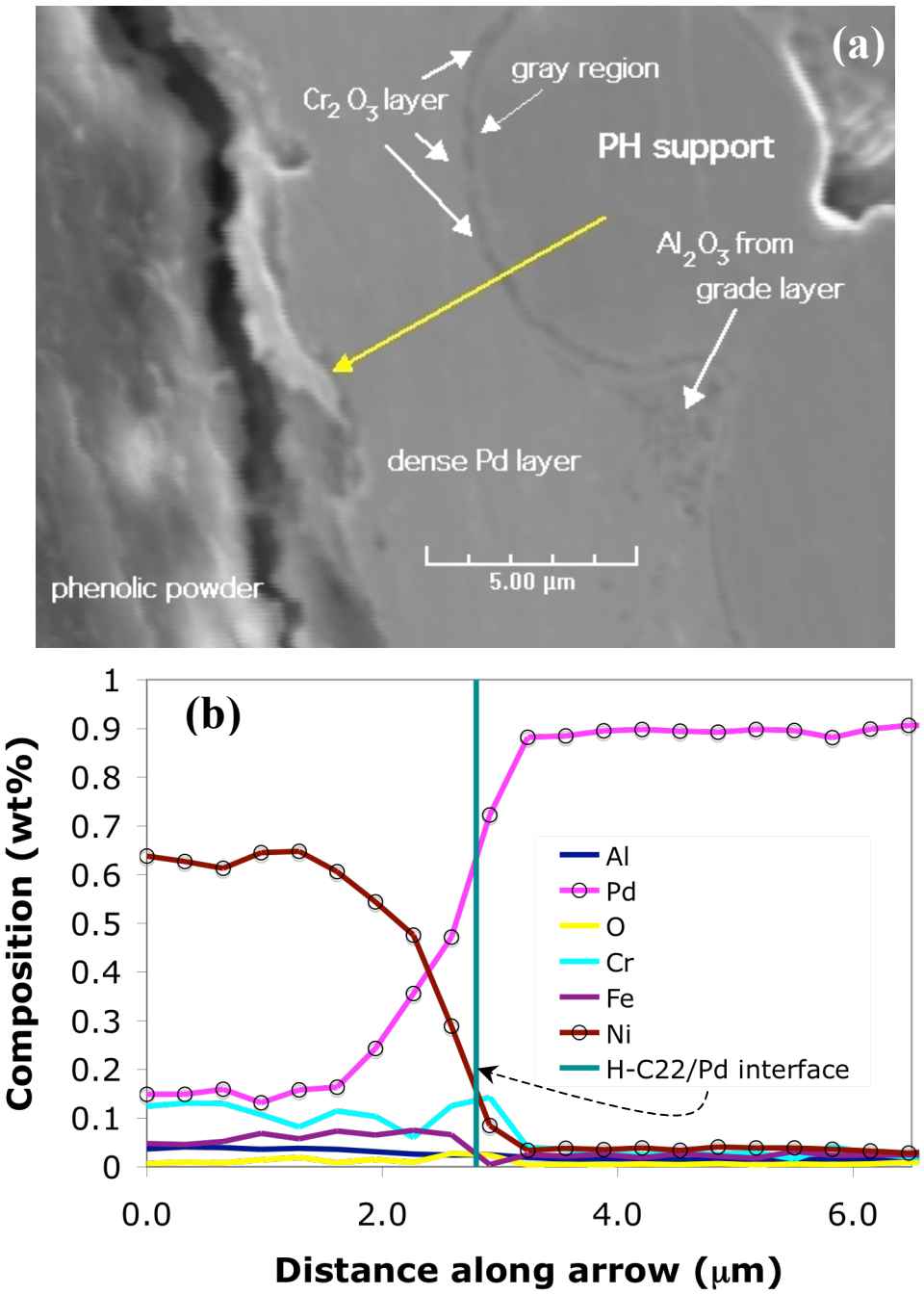

Figure 8-6 (a) Cross-section of Ma-34b after heat-treatment at 600°C in H_2 atmosphere. (b) Elemental composition across the Pd-Oxidized PH interface.

Fe_2O_3 was indeed found to undergo reduction to Fe in H_2 atmosphere in the Pd-Fe_2O_3-Cr_2O_3-PSS composite structure. Also, since the Fe content of PH was only 2-3wt% the driving force for Fe diffusion into the Pd layer was negligible.

8.3.2 Effect of intermetallic diffusion on H_2 permeance

8.3.2.1 Effect on H_2 permeance

Figure 8-7 shows for every temperature the H_2 flux/H_2 $flux_0$ as a function of time for membrane C01-F03. H_2 $flux_0$ was the initial H_2 flux at any given temperature. The initial rate at which the H_2 flux declined was given by the slope of the curve (H_2 flux/H_2 $flux_0$, time) at time t=0. It is clearly seen in Figure 8-7 that the slope of the (H_2 flux/H_2 $flux_0$, time) curved increased as the temperature was increased from 300 to 500ºC in membrane C01-F03. Figure 8-8 shows the H_2 flux/ H_2 $flux_0$ decline as a function of time at 450 and 500ºC for Membrane C01-F04. The initial rate at which the H_2 flux declined, slope of the curve (H_2 flux/H_2 $flux_0$, time) at time t=0, also increased with temperature.

Figure 8-9 shows the H_2 flux/ H_2 $flux_0$ decline for membrane C01-F07. It is interesting to note that the rate at which H_2 flux declined, increased from 300 to 400ºC and then decreased from 400 to 500ºC. The SEM investigation of the surface of membrane C01-F07 revealed the presence of blisters and the detachment of the second Pd layer from the first Pd layer. The selectivity (H_2/He) of the membrane at the end of the characterization process was measured at room temperature and equaled 43. Therefore, the H_2 flux decline at 450, 450 and 500ºC was mostly masked by a large leak development. Since leaks hardly developed at low temperatures, experimental data in the 300-400ºC were taken to be valid.

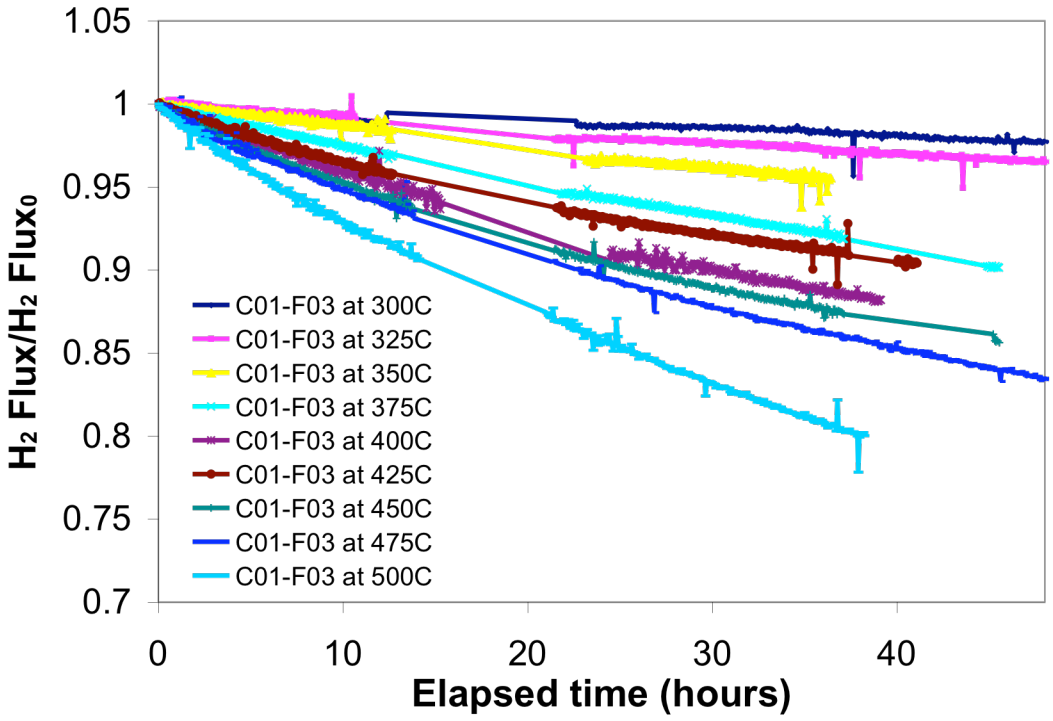

Figure 8-7 H_2 flux/H_2 flux$_0$ as a function of time for all temperatures membrane C01-F03, was tested

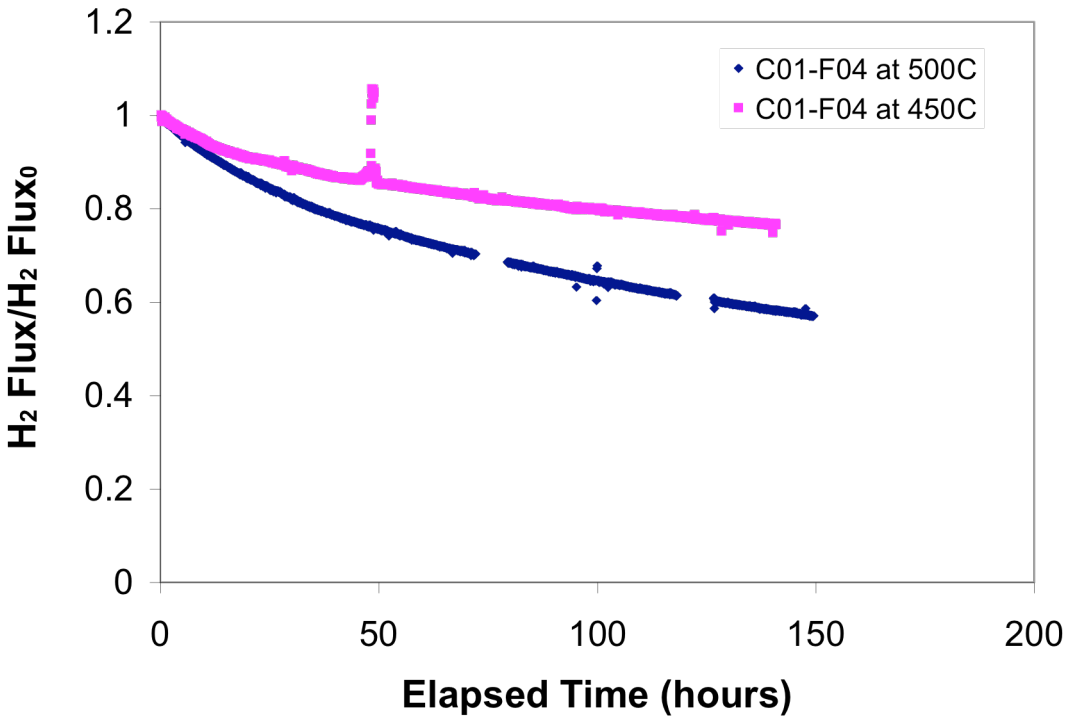

Figure 8-8 H_2 flux/H_2 flux$_0$ vs. time for membrane C01-F04

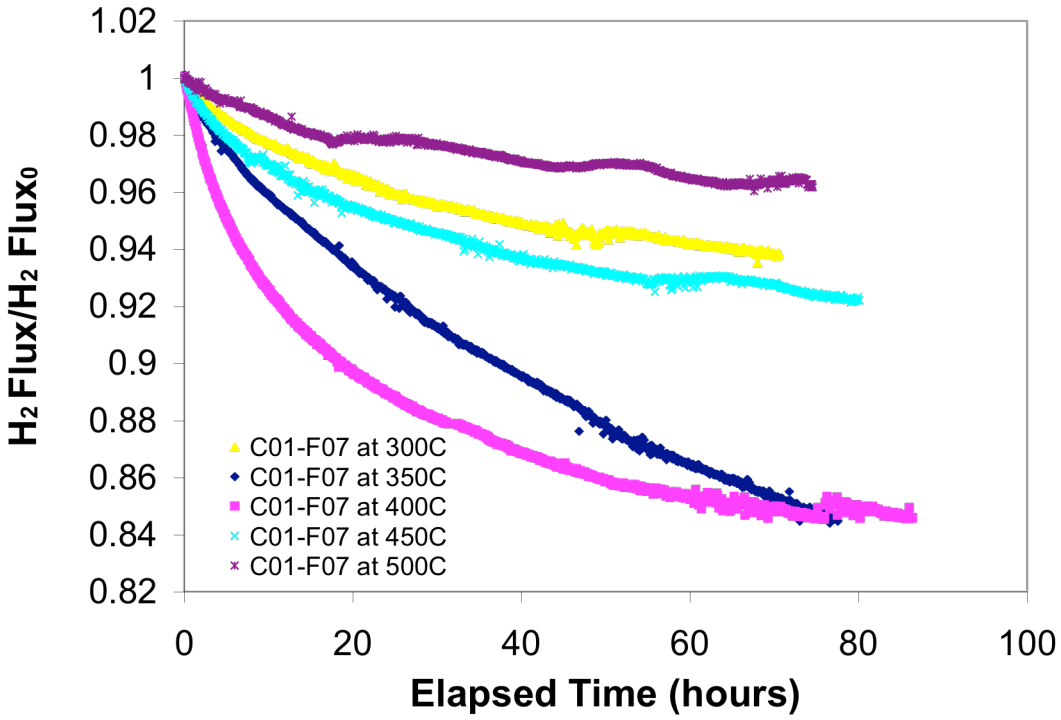

Figure 8-9 H_2 flux/H_2 flux$_0$ vs. time for membrane C01-F07

The H_2 flux of all membranes prepared on oxidized PSS supports (C01-F03, C01-F04, C01-F05, C01-F07 and C01-F08), except for C01-F11 and C01-F11b, started to decrease at a temperature close to 275-300ºC.

The diffusion coefficient of Fe in Pd, $D_{Fe->Pd}$, is equal to $0.18 \cdot \exp(-260000/RT)$ cm^2 s^{-1} (Brandes and Brook, 1998) and the Fe penetration depth into Pd is approximated by $(D_{Fe->Pd}\, t)^{0.5}$ with t in seconds[1] . After 50 hr[2] at 300ºC the penetration depth of Fe into Pd was only $2.54 \cdot 10^{-10}$ m. Hence, Fe diffusion through the lattice of Pd was not responsible for H_2 flux decline at 300ºC seen for membrane C01-F03. After 50 hr at 500ºC the penetration depth of Fe into Pd was $0.3 \cdot 10^{-6}$ m. That is, after 50 hr at 500ºC, the Fe concentration in the Pd layer was higher than around 30wt% up to 0.3 μm, and lower than 30wt% after the 0.3μm (see Figure 8-4(b)). Therefore, at temperatures equal to or higher than 500ºC, the diffusion of Fe through the Pd lattice appeared to be the predominant mechanism leading to the H_2 flux decline seen in all composite Pd-PSS membranes.

Figure 8-10 shows the H_2 flux loss as a function of time for membrane Ma-42 prepared on graded PH supports. Compared to the composite Pd membranes prepared on the PSS support, H_2 flux in Ma-42 membrane decreased at a slower rate. For instance, Ma-42 only lost 10% of its initial H_2 flux after 100 hr at 500ºC. After 100 hr at 500ºC the H_2 flux of Ma-42 became stable.

[1] The penetration depth $(Dt)^{0.5}$ is defined as the distance in the Pd layer from the Pd-PSS interface where the Fe concentration is equal to half of the Fe concentration of the support, which is equal to around 60wt%.

[2] 50 hours was the average time C01-F03 was held at each temperature, see Figure 8-7.

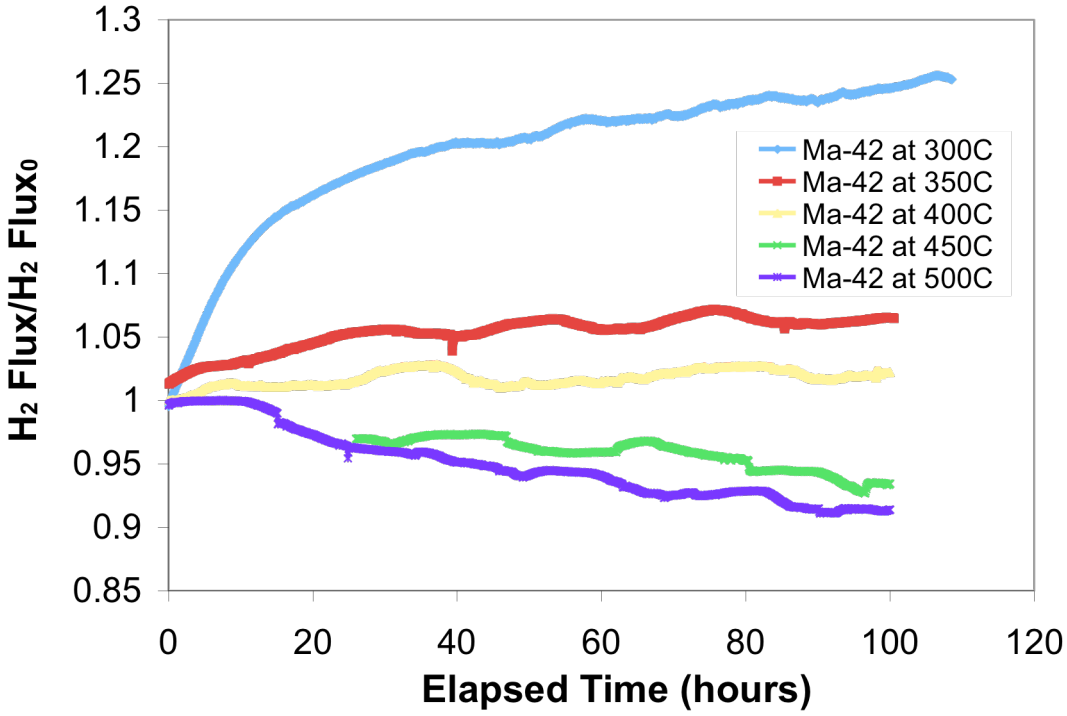

Figure 8-10 H_2 flux loss at different temperatures as a function of time for membrane Ma-42

The H_2 flux of Ma-32/34/42 membranes increased during the first 50-100 hr at 250, 300 and only slightly at 350ºC as seen in Figure 8-10(a). The increase in H_2 flux was not due to leak development since the selectivity of Ma-42 equaled 25000 at 350ºC. This phenomenon, mostly seen in "fresh" composite Pd membrane prepared on graded supports, was described in Section 0.

Table 8-2 lists the temperature at which the H_2 permeance started to decline in each membrane. Membranes prepared on oxidized PSS supports were less stable than membranes prepared on oxidized PH supports. The grade layer (Pd-Al_2O_3) can also act as an intermetallic diffusion barrier since the H_2 permeance of membranes C01-F08/11/11b prepared on graded PSS supports showed greater stability.

Table 8-2 Temperature at which H_2 permeance loss was first recorded for several membranes.

Membrane	Support	Ox.	Graded	Thickness	Temp. of first decrease
C01-F03	0.1 PSS	400	No	32	300
C01-F04	0.1 PSS	none	No	28	300
C01-F05	0.1 PSS	500	No	33	350
C01-F07	0.1 PSS	500	No	23	300
C01-F11	0.1 PSS	500	Yes	15	500
C01-F11b	C01-F11	500	Yes	17	T>500*
Ma-32	0.1 M PH	700	Yes	7.7	T>500
Ma-32b	Ma-32	700	Yes	10	T>500
Ma-34	0.1 MC PH	700	Yes	4	T>500
Ma-34b	Ma-34	700	Yes	8	600
Ma-42	0.1 M PH	700	Yes	5.6	450

*T>500ºC stands for: no H_2 permeance loss was recorded up to 500ºC, which was the maximum temperature the membrane was exposed to

8.3.2.2 Intermetallic diffusion effect on activation energy for H_2 permeation

The H_2 flux decline due to the intermetallic diffusion that occurred during the 50 minutes necessary to perform a 50ºC temperature change at temperatures lower than 550ºC

was negligible compared to the increase of H_2 flux due to the 50ºC temperature change, (see Section 5.4.5). Therefore, it was possible to determine the changes in the activation energy for H_2 permeation as the temperature was increased to 250, 300, 350, 400, 450, 500 and 550ºC. However, at temperatures higher than 550°C, the intermetallic diffusion rate was fast enough leading to a significant H_2 flux decrease during the 50 minutes of the temperature change and no valid activation energy could be determined by the temperature ramp method. The activation energy for H_2 permeation was determined for membrane C01-F05 by measuring H_2 flux (ΔP=1bar) at every temperature change (1:250ºC-300ºC; 2:300ºC-350ºC; 3:350ºC-400ºC; 4:400ºC-450ºC; 5:450ºC-500ºC; 6:500ºC-550ºC; 7:550ºC-600ºC and 8:600ºC-650ºC). Figure 8-11 shows the activation energy values for each temperature interval for membrane C01-F05. The activation energy for H_2 permeation, F_{H2}, increased from 10.5 kJ mol^{-1} in the 250°C-300°C temperature window to 18 $kJmol^{-1}$ at 500°C-550°C. Above 550°C, the activation energy for H_2 permeation, F_{H2}, decreased due to the fact that the H_2 flux loss during temperature change was no longer negligible compared to H_2 flux increase due to temperature increase. In order to measure the activation energy for H_2 permeation, F_{H2}, at temperatures higher than 550-600ºC, membrane C01-F05 was annealed at a maximum temperature of 700°C for one hour and the activation energy for H_2 permeation through a Fe-Cr rich Pd layer was determined while decreasing temperature in one step from 600ºC to 250ºC. The activation energy for H_2 permeation was measured to be 31 $kJmol^{-1}$ in the 250°C-600ºC temperature range, which was consistent with the fact that the E_p for Pd-Fe and Pd-Cr alloys is higher than the E_p for pure Pd (Flanagan et al., 1977; Swansiger et al., 1976).

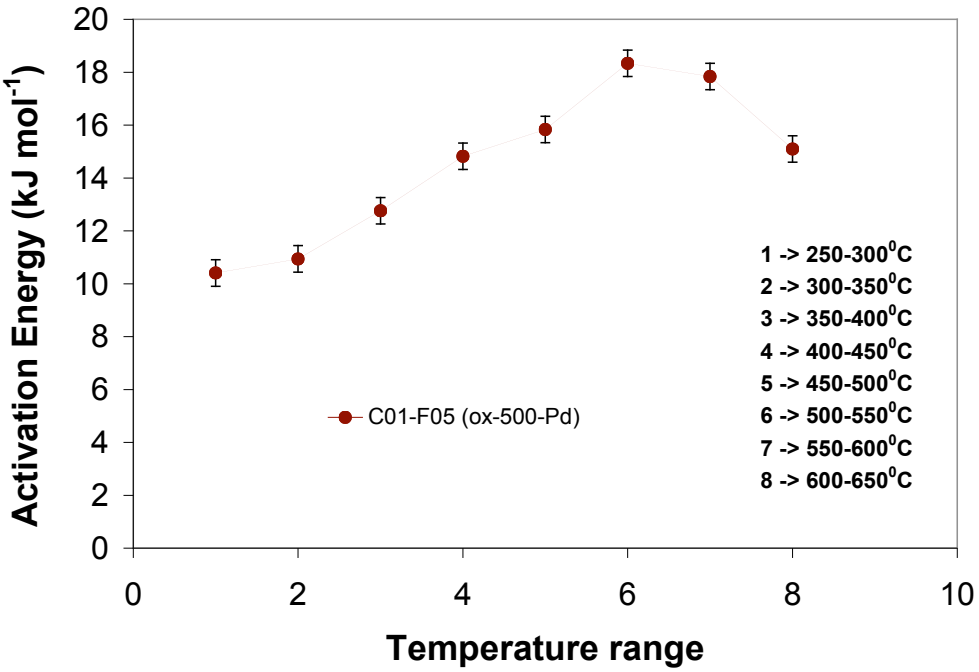

Figure 8-11 Activation energy for H_2 permeation vs. temperature change for membrane C01-F05.

Figure 8-12(a) and (b) show the cross-section micrograph and the elemental composition across the Pd-oxidized PSS interface for membrane C01-F05 after heat-treatment at 700ºC for one hour. The original Pd layer, which had a thickness close to 33μm, showed a Pd-Fe-Cr-Ni alloy layer with a thickness of around 15μm and a rich Pd layer of 20 μm. The 15μm thick Pd-Fe-Cr-Ni alloy layer represented the main resistance for H_2 permeation, thereby explaining the high activation energy found for the H_2 permeation in C01-F05 membrane. Hence, intermetallic diffusion led to the increase of activation energy for H_2 permeation due to the presence of Fe rich Pd alloys at the vicinity of the PSS support.

The activation energies for H_2 permeation of membranes C01-F03, C01-F07, Ma-32, Ma-32b and Ma-34b were also calculated at all temperatures changes and plotted with the values of C01-F05 in Figure 8-13. Membranes C01-F03 and C01-F07 showed a similar trend than C01-F05: an increase in the H_2 permeation activation energy from values of 9-12 kJ mol^{-1} in the 250°C-300°C temperature window to 16-18 kJ mol^{-1} in the 450°C-500°C temperature window. A slight increase in activation energy was consistently noticed after some H_2 flux decline at a given temperature similar to the H_2 flux declines recorded for membranes C01-F03, C01-F04 and C01-F07 seen in Figure 8-7, Figure 8-8 and Figure 8-9.

In Section 5.4.3.2, all composite Pd membranes prepared on graded PH supports (Ma-32/32b/34/34b/41/42) were proven to have mass transfer resistance within their porous support. Therefore, the activation energy for H_2 permeation, F_{H2}, of membranes Ma-32/32b and Ma-34b was lower than the activation energy for H_2 permeation of C01-F03/5/7 membranes as seen in Figure 8-13. All membranes have similar activation energies for H_2 permeation in the 250-300ºC temperature interval.

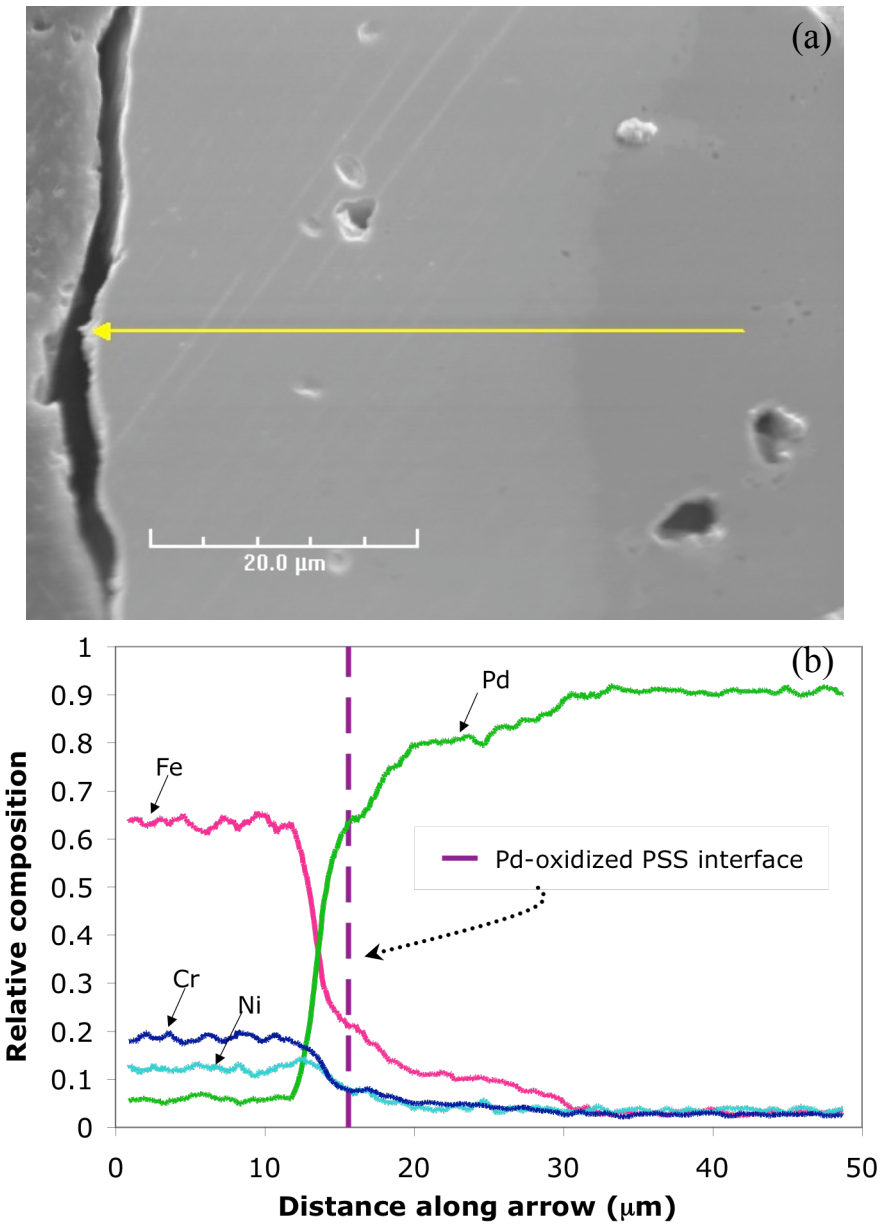

Figure 8-12 (a) Cross-section of C01-F05 after heat-treatment at 700ºC in H_2 atmosphere for 1 hr. (b) Elemental composition across the Pd-Oxidized PSS interface

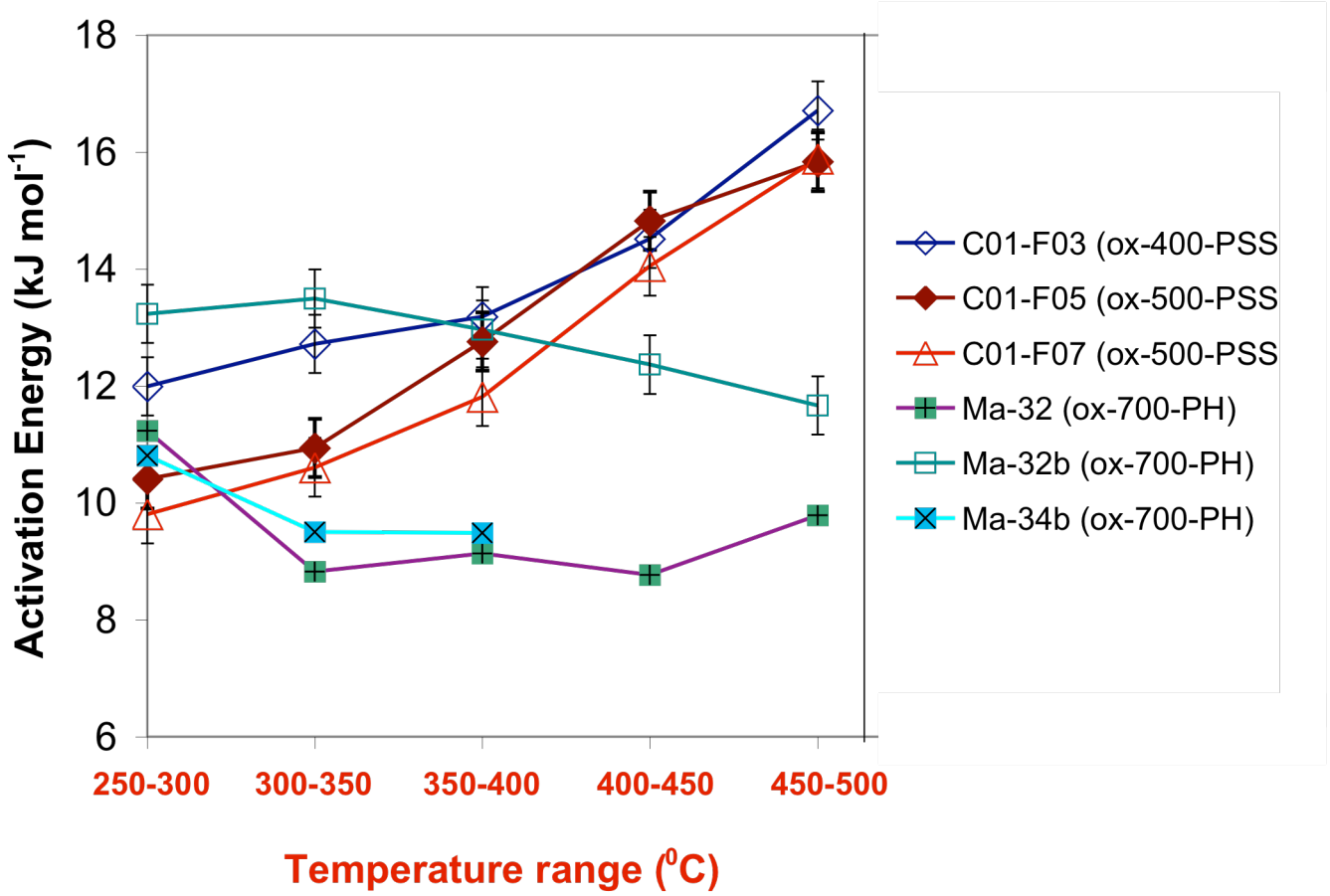

Figure 8-13 Activation energy of H_2 permeation, F_{H2}, determined in several temperature ranges for membranes C01-F03, C01-F05, C01-F07, Ma-32, Ma-32b and Ma-34b

The E_p of C01-F03/5/7 membranes increased with temperature due to the intermetallic diffusion, while the E_p of Ma-32/32b/34b membranes decreased with temperature due to the mass transfer resistance.

It is interesting to note that the activation energies for all membranes determined in the 250°C-350°C temperature range were slightly lower than the average activation energies calculated for Pd foils in Section 4.2.3 and equal to 14.9 $kJmol^{-1}$. As already stated in Section 5.4.5.2 the low activation energies for the H_2 permeation were found at low temperatures in all the composite Pd membranes in this study. The low activation energies for H_2 permeation were due to the H_2 diffusing through Pd grain boundaries (in the nanometers range), leaks (Knudsen and viscous of H_2) and/or in the case where the support represented an important resistance for H_2 permeation as explained in Section 5.4.3.1.

The activation energy of grain boundary diffusion is about 1/2 to 2/3 of the activation energy of lattice diffusion. Therefore, composite Pd membranes having Pd crystallites in the nanometer size were expected to show a lower activation energy for H_2 permeation than the activation energy measured in Pd foils, which had very large Pd crystallites.

All membranes showed high selectivities, especially in the 250-350°C temperature range where defects formation was unlikely. Therefore, the low activation energies for H_2 permeation observed at low temperatures in all composite membranes were not due to leaks. In the case of thick membranes the main resistance to H_2 permeation was "bulk" diffusion, therefore, the mass transfer resistance within the porous support of C01-F03, C01-F05 and C01-F07 did not have any effect on the H_2 permeance. Moreover, their ξ_{250}, defined in Section 5.4.3.2, values were higher than 100. Hence, the small grain sizes

found in all composite Pd membranes affected the activation energy for H_2 permeation at low temperatures.

In summary, intermetallic diffusion led to the increase of the activation energy for H_2 permeation.

8.3.3 Intermetallic diffusion mechanism

In order to clearly understand the diffusion mechanism of elements from the support into the Pd layer, a kinetic approach was undertaken. The rate of the H_2 flux loss of membrane C01-F05 was measured at ΔP=1 bar at different temperatures for long periods of time. The H_2 flux of membrane C01-F05 was stable at 250ºC and 300ºC. However, at 350ºC the H_2 flux of C01-F05 started to decrease. The rate at which the H_2 flux declined increased up to 650ºC. Figure 8-14(a) shows the normalized H_2 flux (H_2 flux divided by the initial H_2 flux) as a function of time for temperatures equal to and lower than 500ºC. Figure 8-14(b) shows the normalized H_2 permeance as a function of time for temperatures higher than 500ºC. The rate at which the H_2 flux declined was calculated by assuming the loss to be linear during the first 50 hr in the low temperature range (T<500ºC). In the high temperature range (T>500ºC) the H_2 flux decline was rapid and measurements were taken within 3 to 10 hr.

Figure 8-15 is the Arrhenius plot of the initial (measured over 3-50 hr) H_2 permeance loss rate for membrane C01-F05. An average activation energy of 25 kJ mol^{-1} can be derived in the 350°C-500ºC temperature range. The activation energy at higher temperatures, 500°C-650ºC was determined to be 168 $kJmol^{-1}$. Due to the high activation energy shown at temperatures higher than 500ºC, the nature of the process with the high activation energy (above 500ºC) was most probably due to the intermetallic diffusion, i.e.

mostly diffusion of Fe from the supports through the lattice of the dense Pd layer and vice versa (Pd diffusing into the lattice of the support).

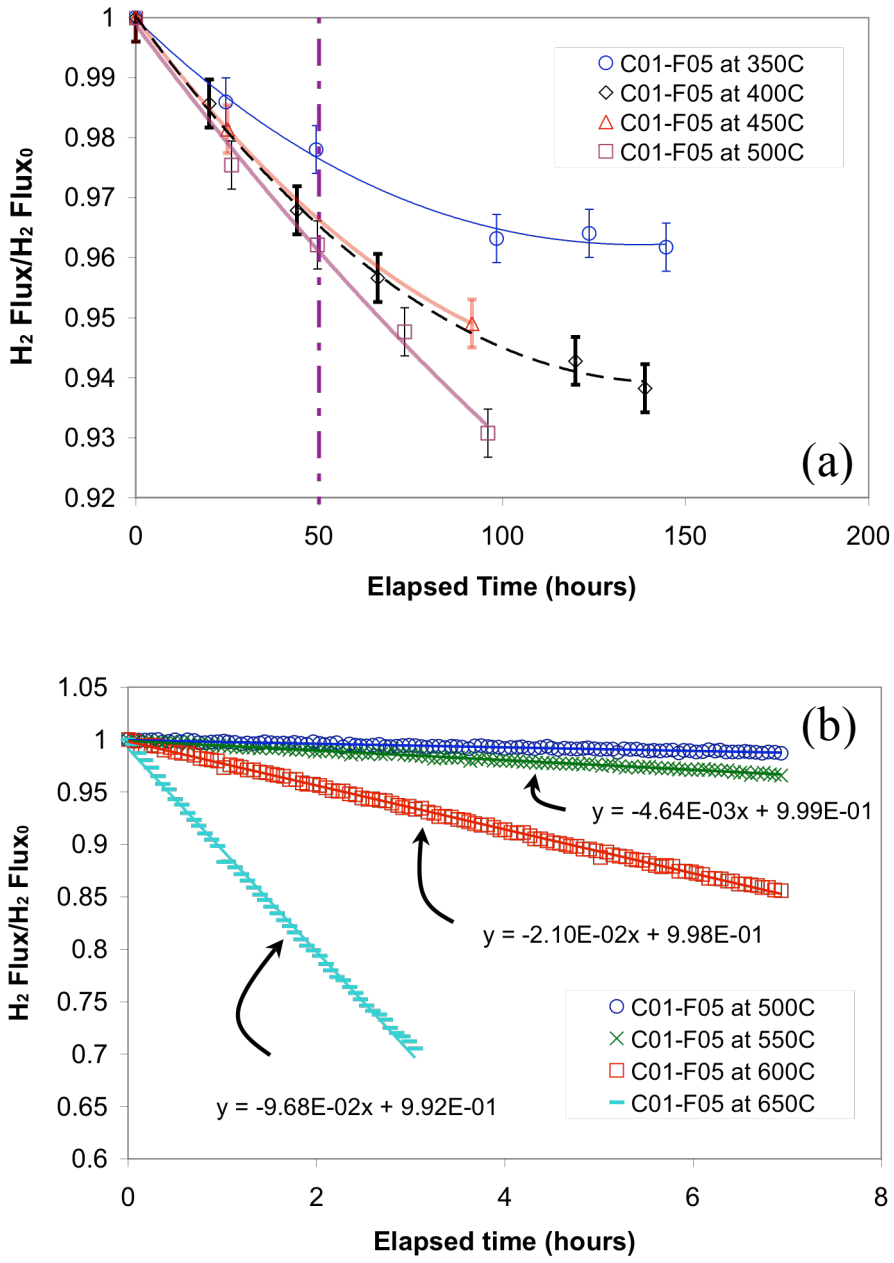

Figure 8-14 H_2 flux loss as a function of time at (a) 350, 400, 450 and 500ºC and (b) 500, 550, 600 and 650ºC for C01-F05 membrane.

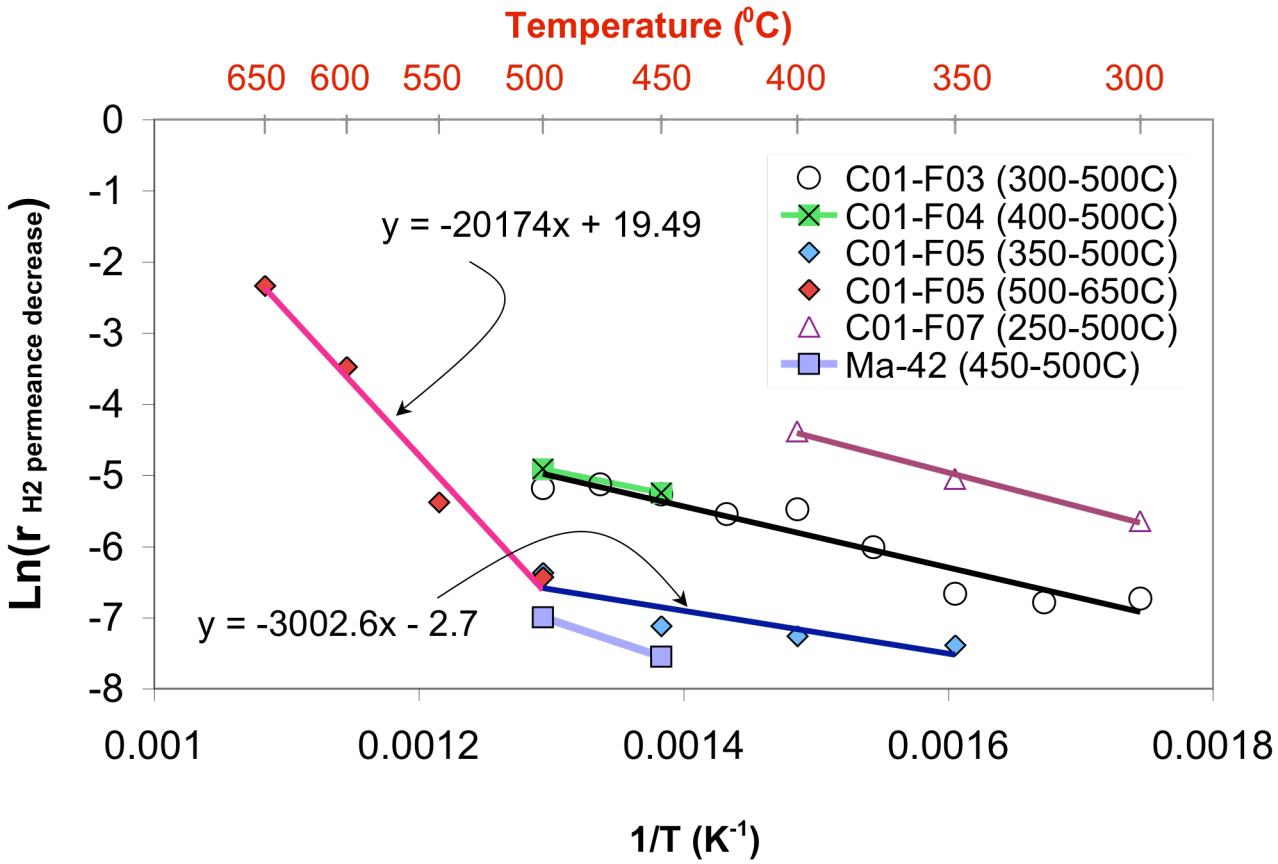

Figure 8-15 Ln(H_2 flux loss rate) as a function of 1/T for C01-F03/4/5/7 and Ma-42 membranes

Indeed, the activation energy for most of the metal-metal lattice diffusion couples is 100-300 kJ mol^{-1}. The initial H_2 permeance loss rate was also measured for C01-F03 (see Figure 8-7(a)), C01-F04 (see Figure 8-7(b)), C01-F07 in the 300-400ºC temperature range (see Figure 8-7(c)) and Ma-42 (see Figure 8-10(b)). The Arrhenius relations of the H_2 permeance loss for membranes C01-F03/4/7 and Ma-42 were also plotted in Figure 8-15. The activation energy for the H_2 permeance decline is listed for all membranes in Table 8-3.

Table 8-3 Activation energy for H_2 flux loss rate for all membranes in Figure 8-15 in the low (T<500ºC) and high (T>500ºC) temperature range

Membrane	Ea below 500ºC (kJ mol^{-1})	Ea above 500ºC (kJ mol^{-1})
C01-F03	35.8	
C01-F04	31.4	
C01-F05	**25**	**167.7**
C01-F07	40.4	
Ma-42	51.3	

The mechanism that took place at lower temperatures (T<500ºC) was significantly different from lattice intermetallic diffusion. The H_2 permeation loss was characterized by a low activation energy in the 300°C-500ºC temperature window for all membranes.

Possible mechanisms with low activation energies are: grain boundary diffusion of Fe, Cr or Ni in between the Pd grains (the activation energy for grain boundary diffusion is usually equal to 10-50 kJ mol^{-1}), Pd grain growth leading to a decrease in H_2 permeation (20-60 kJ mol^{-1}) or reduction of the Fe_2O_3 oxide, formed by the oxidation in air, and subsequent lattice or grain diffusion of Fe into Pd as seen in Section 8.3.1.2.

Figure 8-16 (a) and (b) show a composite (secondary electrons image + backscatter image) micrograph of membrane C01-F03 cross-section at low and high magnification respectively. The sample was slightly etched with diluted aqua regia for 10 seconds in order to generate more contrast and see the microstructure. Pd is slowly etched by diluted aqua regia, however, Fe is readily etched by aqua regia. Hence, the etchant preferentially dissolved the regions in the Pd layer having a high Fe content.

The structure of the outermost part of the Pd layer seen in Figure 8-16 (a) appeared quite uniform while the structure of the innermost part (close to the PSS support) appeared to be grainy. A dashed grey line separates the highly etched part of the Pd layer from the non-etched part of the layer. The fact that the outermost part of the Pd layer was not etched and the innermost part of the Pd layer was etched indicated that the Pd layer was richer in Fe at the vicinity of the support. Therefore, the etchant preferentially dissolved the innermost part of the Pd layer. White arrows in Figure 8-16(a) point at grey regions. The grey color is due to the presence of Fe and it appears that in those regions Fe diffused through the lattice of Pd.

Figure 8-16 (b) is a high magnification micrograph of the region of the Pd layer adjacent to the PSS support. The etchant clearly reveals Pd grains and Pd grain boundaries. The Pd grains had sizes in the order of one micron. Also, since the etchant preferentially removed Fe rich regions it can be concluded that the dark grain boundaries seen in Figure 8-16(b) were rich in Fe. Also, in the backscatter mode, dark regions corresponded to low Z elements, therefore, the Fe concentration along the grain boundaries was very high.

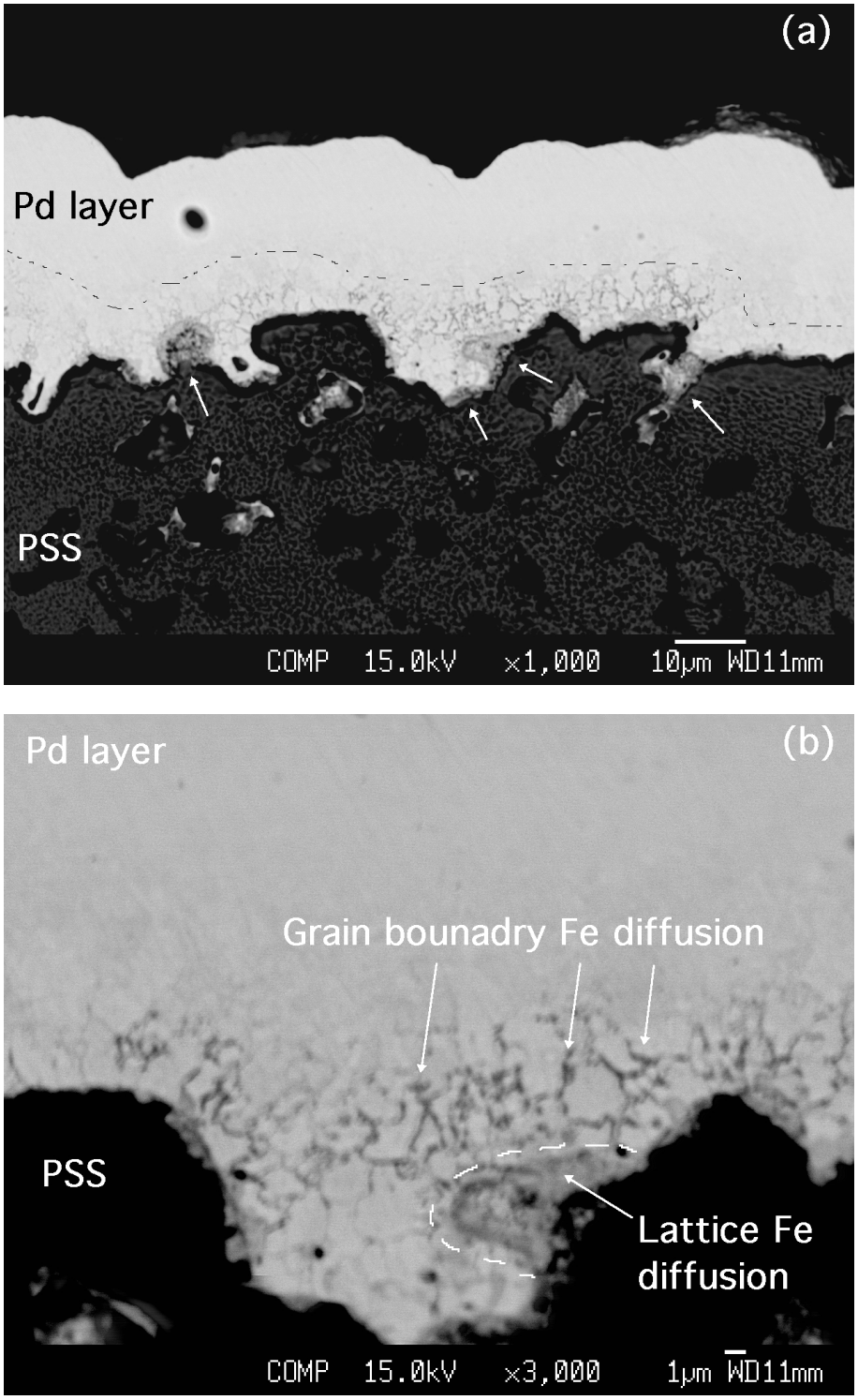

Figure 8-16 Composite image (secondary electron and backscatter of C01-F03 membrane cross-section at (a) low magnification and (b) high magnification of the same area. (Pictures taken by Larry Walker at the html, ORNL, TN)

In fact, the dark grain boundaries indicate that Fe diffused along the grains boundaries rather than through the Pd lattice. Membrane C01-F03 was characterized up to 500ºC, which was the temperature limit for the low activation energy mechanism leading to H_2 flux decline in composite Pd membranes.

In the 250-500ºC interval, the average activation energy for H_2 flux declined equaled 36.8 kJ mol^{-1}, which was consistent with the activation energy for grain boundary diffusion (50kJ mol^{-1}). Hence, most probably, the H_2 flux decline in the low temperature (230-400ºC) range seen in many membranes was due to Fe diffusion through the Pd grain boundaries.

If the presence of Fe within the Pd grain boundaries affected the H_2 permeance, part of the H_2 permeating through the Pd layer must have diffused through the grain boundaries. The activation energy for H_2 permeation in composite Pd membranes was relatively low in the 250-300ºC (see Section 5.4.5.2), which was found to be consistent with H_2 flowing through grain boundaries. Although H_2 diffuses faster in the grain boundaries (Janßen et al., 1997), it is still not known if and how the size of Pd grains affects the H_2 permeance of a composite Pd membrane. The fact that the presence of Fe within the Pd grain boundaries led to H_2 flux decrease attests to the fact that some H_2 diffused through the grain boundaries.

8.4 Conclusions

The oxidation of 316L PSS supports at a temperature lower than 500ºC resulted in a thin Cr_2O_3 layer. When the oxidation temperature was higher than 600ºC, a PSS-thin Cr_2O_3-thick Fe_2O_3 composite structure was formed. Oxidation of PH supports at 900ºC resulted in a thin (several microns) Cr_2O_3 layer. Fe_2O_3 oxide was reduced to metallic Fe,

even when covered with Pd, when the composite Pd-Fe_2O_3-Cr_2O_3-PSS structure was put in H_2 atmosphere at low temperatures. Experimental evidence showed that Cr_2O_3 was not reduced in H_2 atmosphere. PH supports had a stronger tendency to develop thicker Cr_2O_3 layer with no Fe_2O_3 layer at the surface. PH supports showed better properties in preventing intermetallic diffusion. In composite Pd-PSS membranes the intermetallic diffusion led to a decrease of H_2 permeance and an increase of activation energy for H_2 permeation from 10-12 $kJmol^{-1}$ to 16-18 $kjmol^{-1}$ in agreement with the higher activation energies for H_2 permeation shown by Pd-Fe and Pd-Cr alloys. The intermetallic diffusion occurred according to a process with low activation energy (25-50$kJmol^{-1}$) at low temperatures (300°C-500ºC) and a process with a high activation energy (170$kJmol^{-1}$) at high temperatures (500°C-650ºC). The process at high temperatures was demonstrated to be lattice intermetallic diffusion i.e. diffusion of Fe through the lattice of Pd and vice versa. The mechanism involved in the low temperature range was the diffusion of Fe within the Pd grain boundaries.